Functional characterization of aromatic amino acid aminotransferase involved in 2-phenylethanol biosynthesis in isolated rose petal protoplasts

Title “Functional characterization of aromatic amino acid aminotransferase involved in 2-phenylethanol biosynthesis in isolated rose petal protoplasts”

Short running title: Rose phenylalanine amino acid amino transferase

Corresponding author:

Name: Naoharu Watanabe

Mailing address: Graduate School of Science and Technology, Shizuoka University, 836 Ohya, Suruga-ku, Shizuoka 422-8529, Japan

Tel/Fax: +81-54-238-4870.

E-mail address: acnwata@ipc.shizuoka.ac.jp

Functional characterization of aromatic amino acid aminotransferase involved in 2-phenylethanol biosynthesis in isolated rose petal protoplasts

Hiroshi Hirata[1,5], Toshiyuki Ohnishi[2,5], Haruka Ishida[3], Kensuke Tomida[3], Miwa Sakai[3], Masakazu Hara[4] and Naoharu Watanabe[1,5,*]

[1]Graduate School of Science and Technology, Shizuoka University, 836 Ohya, Suruga-ku, Shizuoka 422-8529, Japan

[2]Division of Global Research Leaders, Shizuoka University, 836 Ohya, Suruga-ku, Shizuoka 422-8529, Japan

[3]Faculty of Agriculture, Shizuoka University, 836 Ohya, Suruga-ku, Shizuoka 422-8529, Japan

[4]Department of Applied Biological Chemistry, Shizuoka University, 836 Ohya, Suruga-ku, Shizuoka 422-8529, Japan

[5]These authors contributed equally to this work.

* Corresponding author

Tel/Fax: +81-54-238-4870.

E-mail address: acnwata@ipc.shizuoka.ac.jp

ABSTRACT

In rose flowers, 2-phenylethanol (2PE) is biosynthesized from L-phenylalanine (L-Phe) *via* phenylacetaldehyde (PAld) by the actions of two enzymes, pyridoxal-5'-phosphate (PLP)-dependent aromatic amino acid decarboxylase (AADC) and phenylacetaldehyde reductase (PAR). We here report that *Rosa* 'Yves Piaget' aromatic amino acid aminotransferase produced phenylpyruvic acid (PPA) from L-Phe in isolated petal protoplasts. We have cloned three full length cDNAs (*RyAAAT1-3*) of aromatic amino acid aminotransferase families based on rose EST database and homology regions. The RyAAATs enzymes were heterogeneously expressed in *E. coli* and characterized biochemically. The recombinant RyAAAT3 showed the highest activity toward L-Phe in comparison with L-tryptophan, L-tyrosine, D-Phe, glycine, and L-alanine, and showed 9.7-fold higher activity with L-Phe rather than PPA as a substrate. RyAAAT3 had an optimal activity at pH 9 and at 45-55 ^{o}C with α-ketoglutaric acid, and was found to be a PLP dependent enzyme based on the inhibition test using Carbidopa, an inhibitor of PLP-dependent enzymes. The transcript of *RyAAAT3* was expressed in flowers as well as other organs of *R.* 'Yves Piaget'. RNAi suppression of *RyAAAT3* decreased 2PE production, revealing the involvement of *RyAAAT3* in 2PE biosynthesis in rose protoplasts and indicating that rose protoplasts have potentially two different 2PE biosynthetic pathways, the AADC

route and the new route *via* PPA from L-Phe.

Keywords

2-Phenylethanol; Aromatic amino acid aminotransferase; Biosynthesis; Phenylpyruvic acid; Rose

Abbreviations: 2PE, 2-phenylethanol; AAAT, aromatic amino acid aminotransferase; AADC, aromatic amino acid decarboxylase; AspAT, aspartate aminotransferase; AlaAT, alanine aminotransferase; *E. coli*, *Escherichia coli*; PAld, phenylacetaldehyde; PAR, phenylacetaldehyde reductase; L-Phe, L-phenylalanine; PheAT, phenylalanine aminotransferase,; PLP, pyridoxal-5'-phosphate; PPA, phenylpyruvic acid; TrpAT, tryptophan aminotransferase; TyrAT, tyrosine aminotransferase

Introduction

2-Phenylethanol (2PE) is one of the prominent scent compounds produced by Damask roses (Hayashi et al, 2003; Sakai et al., 2007; Yang et al, 2009), and in various fruits such as strawberry, tomato and grape varieties (Aubert et al., 2005). 2PE and phenylacetaldehyde (PAld) contribute toward characteristic flavors in wine and cheese (Marilley and Casey, 2004) producing a pleasantly sweet, flowery note at low concentrations, while PAld is nauseating and unpleasant at high levels (Tadmor et al., 2002). The world's annual production of 2PE is estimated to be approximately 10,000 tons in 2010 (Schwab et al., 2008; Hua and Xu, 2011).

2PE is biosynthesized from L-phenylalanine (L-Phe) with pyridoxal-5'-phosphate (PLP)-dependent aromatic amino acid decarboxylases (AADC) and phenylacetaldehyde reductases (PAR) in *planta* (Fig. 1A) (Sakai et al., 2007). AADC transformed L-Phe to PAld *via* the Schiff base, which was formed by a reaction between the amino group of L-Phe and a formyl group of PLP. PAld was also synthesized by plant PAld synthase (PAAS), a member of the AADC family, in *Petunia hybrida* (Kaminaga et al., 2006) and by AADC in *Solanum lycopersicum* (Tieman et al., 2006) and *Arabidopsis* (Gutensohn et al., 2011).

PAld is converted to 2PE by the action of PAR (Tieman et al., 2007; Chen et al., 2011). Thus, 2PE is synthesized from L-Phe *via* PAld by the action of both enzymes,

AADC and PAR in plants.

Microorganisms biosynthesize 2PE from L-Phe *via* phenylpyruvic acid (PPA), called 'Ehrlich pathway' (Ehrlich, 1907), while there is no report about the Ehrlich pathway in *planta* so far. In microorganisms, the amino acid metabolism has been studied in detail, and it has been reported that aminotransferases play a critical role in forming the corresponding keto-acids that serve as substrates for multiple biochemical reactions (Marilley et al., 2004).

Recently it has been reported that PAld and 2PE emission increased when PPA is administered to melon (*Cucumis melo)* cubes (Gonda et al., 2010). *C. melo* aromatic amino acid aminotransferase (AAAT) cDNA was identified from melon EST database and it was confirmed that *C. melo* AAAT converted L-Phe and L-tyrosine to PPA and 4-hydroxyphenylpyruvic acid, respectively. We hypothesize that in rose petals an alternative biosynthetic pathway to produce 2PE from L-Phe *via* PPA exists, the Ehrlich pathway. To confirm the 2PE biosynthetic pathway *via* PPA and identify AAAT in rose petals, we have first used the rose petal protoplasts for feeding experiments with stable isotope-labeled precursors. Tracer experiments in native plants with stable isotope-labeled precursors have long been used to uncover biochemical pathways (Boatright et al., 2004; Hayashi et al., 2004). However, several parameters such as the feeding method, environmental factors, and difference between

individual plants may influence the elucidation of biochemical pathways of target compounds and their quantitative analysis. In particular, comparatively high concentrations of labeled precursors like amino acids and organic acids are used to enhance the visualization of target compounds, which may lead to false results. Additionally, we encountered the limitations of detecting the intermediates of metabolic pathways due to the dilution of isotope-labeled compounds with endogenous metabolites (Sayama, 2008). Based on the above considerations, we previously developed a simple and controllable approach to elucidate the biosynthesis of 2PE in rose using isolated rose petal protoplasts and confirmed the incorporation of ^{13}C-labeled shikimic acid into 2PE (Yang et al., 2009). Although isolated protoplasts are an artificial system, this model should reveal some fundamental information regarding the biogenesis of 2PE due to the higher conversion rate of exogenously applied precursors within a short incubation period.

Here we report the data obtained by feeding of L-[$^{2}H_{8}$]Phe to protoplasts, which resulted in the conversion to [$^{2}H_{7}$]PPA within a short period. Followed by the detection of [$^{2}H_{7}$]PPA after the feeding with L-[$^{2}H_{8}$]Phe, we have cloned AAATs from rose petals and identified three full length cDNAs of rose AAATs (RyAAAT1-3). Furthermore we characterized biochemically the recombinant RyAAATs, catalyzing the transamination from L-Phe to PPA in 2PE biosynthesis in isolated rose protoplasts.

Material and methods

Plant material and protoplasts feeding experiments

Cut flowers of Damask rose *Rosa* 'Yves Piaget', grown in the green house, were purchased from Ichikawa Rosary in Mishima-City, Japan. The stages of floral growth and the preparation of protoplasts have been described previously (Hayashi et al., 2004; Yang et al., 2009). L-Phe and L-[$^2H_8$]Phe (2.5 μmol) were dissolved in protoplast buffer and added to the protoplasts. The protoplasts were incubated at 30 ^oC for 24 h. [$^2H_7$]PPA was extracted and characterized by LC-MS. For 2PE analysis, ethyldecanoate in methanol (1.55 nmol) was added as an internal standard. The volatiles were extracted twice with 700 μL of hexane-ethyl acetate (1:1, v/v). The organic layer was dried over Na_2SO_4 and subjected to GC-MS analyses.

Chemicals

L-[2,3,3,2',2,'4',5',6'-$^2H_8$]Phe (98 atom% ^2H) was purchased from Sigma Aldrich. All the other chemicals were of the highest grade commercially available from Wako Pure Chemicals (Osaka, Japan) and Sigma Aldrich (Tokyo, Japan), unless noted otherwise.

Determination of [$^{2}H_{7}$]PPA by LC-MS

The protoplasts were administered with L-[$^{2}H_{8}$]Phe (2.5 μmol, 24 h at 30 ^{o}C) and then lyophilized. The lyophilized powder was dissolved in 15 mL Milli-Q water and applied to an SPE cartridge (Supelclean™ ENVI-Chrom P SPE Tube, 500 mg). The cartridge was washed with 6 mL of water and eluted with 6 mL of acetonitrile. The acetonitrile fraction was concentrated *in vacuo* and redissolved in 100 μL 5% acetonitrile. An aliquot of each sample was subjected to the LC-MS analysis. An authentic sample of PPA showed retention time of 6.66 min and *m/z* 163 $[M-H]^{-}$ while [$^{2}H_{7}$]PPA showed a retention time of 6.62 min and *m/z* 170 $[M-H]^{-}$.

Preparation of crude enzymes from the flowers of *R.* 'Yves Piaget'

Preparation of crude enzymes has been described previously (Sakai et al., 2007). The detailed conditions are described in the 'Supplementary information'.

Assay of L-Phe transamination activity

Reaction mixture (150 μL) containing 10 mM L-Phe, 10 mM α-ketoglutaric acid and 30 μL enzyme solution in a 0.5 M Tris-HCl buffer (pH 9.0) was incubated at 45 ^{o}C for 10 min. The reaction was stopped by adding an equal volume of acetonitrile after adding 200 nmol L-[$^{2}H_{8}$]Phe as an internal standard. The sample was subjected

189 to centrifugation (20,000 *g*, 10 min, 4 °C), and filtered (Millex LH, Millipore) prior to
190 analysis by LC-MS. For the reverse reaction 10 mM PPA and 10 mM L-glutamic acid
191 were used instead of L-Phe and α-ketoglutaric acid identical reaction conditions.
192
193 Assay of PPA decarboxylation activity
194 Reaction mixture (200 µL) containing 5 mM PPA, 0.1 mM Thiamine
195 diphosphate, 0.5 mM $MgCl_2$, 100 µl crude enzyme solution in a 0.2 M citrate buffer
196 (pH 6.0), and was incubated at 35 °C for 2 h. Then 3-phenylpropion aldehyde (23.3
197 pmol) dissolved in ethanol (as an internal standard) was added to reaction mixture and
198 PPA was extracted with a 400 µl mixture of hexane and ethylacetate (1:1 v/v). The
199 organic phase was dried over anhydrous Na_2SO_4 and analyzed by GC-MS.
200
201 LC-MS analysis
202 The LC-MS separation module was equipped with a SHIMADZU SPD-M10A
203 PDA and LC-MS2010A. The separation was performed on a YMC-Pack ODS AQ
204 column (2.0 × 150 mm, 5.0 µm, YMC) connected to a GUARD CARTRIDGE
205 CAPCELL C18 UG120 (4.0×10 mm, SHISEIDO). The solvents used were A: 5 mM
206 ammonium acetate (pH 7.0), and B: acetonitrile (Dorman et al., 2008). The gradient
207 was developed by increasing the latter from 5% to 90% in 13.5 min, then holding the

concentration constant for 2.5 min with a flow rate of 0.2 mL/min at 40 °C. The PDA detection range was 190 to 370 nm and the MS detection system was operated in the negative ionization mode with a scan range of *m/z* 100–300. The tuning parameters were as follows: capillary voltage 3.5 kV; cone voltage 20 V; source block temperature 120 °C; and desolvation temperature 350 °C.

GC-MS analysis

The volatile compounds were analyzed as described previously (Yang et al., 2009). The details conditions are described in the 'Supplementary information'.

EST database of rose flowers

Rose flower petals (stage 5, 5 g) were subjected to RNA extraction with RNeasy Plant Mini Kit (QIAGEN) and then purified to obtain mRNA with Oligotex-dT30 mRNA Purification Kit (TaKaRa). EST database was constructed by Dragon Genomics Center (TaKaRa Bio, Japan).

Molecular cloning of RyAAATs and expression in *E. coli.*

Degenerate RyAAATs primers (Supplementary Table 1) were designed using conserved regions among aspartate aminotransferases (AspATs, GenBank association

numbers: NP001031394, NP850022, NP565529, AAQ54557, BAD54126, BAD27593, BAD19094, NP178152, NP177890, NP001118421, and NP180654), and the tyrosine aminotransferase (TyrAT) EST (CF349437 in *R.* hybrid cultivar) (Guterman et al., 2002) and the alanine aminotransferase (AlaAT) (in-house rose EST database). These cDNAs of RyAAAT candidates were amplified by RT-PCR from total RNA extracted from stage 3 rose petals. The PCR products were cloned into the pCR2.1 TA-Cloning vector (Invitrogen) and sequenced, and then 3 different sequences of RyAAAT candidates were subcloned into the pET28a expression vector, which contains an N-terminal histidine tag (Novagen). The cloned genes were expressed in *E. coli* BL21(DE3) cells grown in LB medium with 50 μg/mL kanamycin at 37 ^{o}C. Protein production was induced by the addition of 1 mM IPTG (TaKaRa). After incubation at 27 ^{o}C for 24 h, the crude proteins were extracted with 20 mM potassium phosphate buffer (pH 7.5) containing 0.75 mM PLP and 0.1% Triton X-100 (Extraction buffer). The proteins were purified with HisTrap HP column (GE Healthcare) equilibrated with the extraction buffer (without Triton X-100) and eluted using a linear 0–0.75 M imidazole gradient in the same buffer. Protein concentrations were determined using Bradford reagents (Bio-Rad) with bovine serum albumin as the standard.

RyAAAT3 substrate specificity

The substrate specificity for transamination of RyAAAT3 was determined by quantification of the various keto-acid products and the reduction of L-alanine and glycine. The details are described in the 'Supplementary Information'.

Inhibition of PLP-dependent enzymes with Carbidopa

We have reported rose AADC expression in *E. coli* (Sakai et al., 2007). The crude proteins were extracted with 20 mM potassium phosphate buffer (pH 7.5) containing 1 mM PLP and 0.1% CHAPS. The proteins were purified as described in RyAAATs expression. AADC assay mixtures (400 µL) containing 4 mM L-Phe and 200 µL enzyme solution in a 0.2 M potassium phosphate buffer (pH 8.0) were incubated at 35 ^{o}C for 1 h, and then PAld was extracted and analyzed as described above.

Inhibition assays of AADC and AAAT with Carbidopa (Burkhard et al., 2001; Bertoldi et al., 2002) were performed as decarboxylation and transamination assay with or without carbidopa dissolved in dimethylsulfoxide (DMSO) to make a final concentration of 5%.

Transcription analysis of *RyAAAT3*

Total RNA was extracted from various tissues derived from three different plants of *R.* 'Yves Piaget' at stage 4. RT-PCR was performed using primer sets for *RyAAAT3* and 18S *rRNA* (Ambion) as a house keeping gene. Competitor primers for 18S *rRNA* were used to avoid excess amplification of the 18S *rRNA*. The ratio of 18S *rRNA* primers and competitor primers was 4:6 (v/v). The transcripts were visualized on a 1% agarose gel stained with ethidium bromide and the amplification curves were at linear process as confirmed at various cycles. *RyAAAT3* primers are listed in Supplementary Table 1.

RNAi suppression experiments

Two kinds of double strand RNA (dsRNA) were prepared based on *RyAAAT3* partial sequences. The dsRNA of RyAAAT3 were synthesized at positions 56-701 of 1266 bp using the T7 RiboMAX System (Promega) and specific primers (Supplementary Table 1), and annealed by incubation at 70 ^{o}C for 10 min (An et al., 2003; 2005). The rose protoplasts (3×10^{5} cells in 200 µL protoplast buffer) were transfected with 75 µg dsRNA using an equal volume of 40% polyethylene glycol-calcium solution (PEG 6000, Fluka) (Sheen, 2001). After incubation for 24 h at 30 ^{o}C, 2.5 µmol L-Phe was added to the protoplasts and they were incubated for another 24 h at 30 ^{o}C. PPA was not detected in the protoplasts, and PAld was detected in low level.

The variation of PAld was too large due to its quick conversion to 2PE in the protoplasts, and therefore the effects of RNAi were evaluated based on the amounts of 2PE. 2PE extraction and GC-MS analysis were carried out as described in the section, 'GC-MS analysis'. Effect of Ry*AAAT3* knockdown was confirmed by RT-PCR as described above.

Results

L-Phe was converted to PPA, and PAld was produced from PPA

To confirm the transamination from L-Phe to PPA in rose petal protoplasts (Fig. 1B), we analyzed [$^2H_7$]PPA by LC-MS after administration of L-[$^2H_8$]Phe to rose petal protoplasts. Authentic PPA (*m/z* 163 $[M-H]^-$) was detected at a retention time (6.66 min), together with an ion peak detected at 6.62 min of *m/z* 170 $[M-H]^-$ for [$^2H_7$]PPA (Fig. 1C). These results demonstrated that PPA was biosynthesized in protoplasts from L-Phe.

We also determined the transamination activity from L-Phe to PPA and conversion from PPA to PAld in the crude enzymes prepared from rose petals. PPA was detected by LC-MS based on the detection of peaks of the ion trace at *m/z* 163 $[M-H]^-$ with the same retention time of authentic PPA (Fig. 2A), revealing that L-Phe was converted to PPA by the enzymes in the *R.* 'Yves Piaget'. Furthermore, we

303 detected PAld production in the crude enzymatic assay mixture with PPA as a
304 substrate by GC-MS (Fig. 2B), revealing that PPA was converted to PAld, precursor
305 of 2PE.
306
307 Full lengths of three RyAAATs were determined and RyAAAT3 showed AAAT
308 activity with L-Phe
309 Blast searching and degenerate PCR cloning from rose petals gave us three EST
310 candidates of RyAAAT putatively catalyzing transamination of L-Phe. We separately
311 obtained three independent full length cDNAs by 3', 5'-RACE PCR. To elucidate
312 whether these cDNAs (RyAAAT1, RyAAAT2 and RyAAAT3) encode functional
313 enzymes the cDNAs were transferred a position vector for expression in *E. coli*. We
314 purified the expressed enzymes and evaluated the activity based upon PPA production.
315 One of candidates (RyAAAT3), homologous to TyrAT, showed PPA production
316 activity with L-Phe (Fig. 3A,B, Supplementary Fig 1). However the other two
317 RyAAAT1 and 2 homologous to AspAT and AlaAT hardly showed any PPA
318 production (Supplementary Fig. 2). Therefore we focused on RyAAAT3 which is a
319 421 amino acid protein with a calculated average molecular weight of 46.3 kDa and
320 pI of 6.28 (GenBank/EMBL accession number AB669189), and includes a
321 aminotransferases family-I PLP attachment site (SLSKrwLVpGWRLG) and the

highly conserved residue (arginine 393) in family I for the binding of these enzymes substrates (Huang et al., 2008; Yennawar et al., 2001). The deduced amino acid sequences of RyAAAT3 showed 78% similarity to *C. melo* AAAT. I*n silico* analysis by TargetP 1.1 (http://www.cbs.dtu.dk/services/TargetP/), ChroloP 1.1 (http://www.cbs.dtu.dk/services/ChloroP/), SignalP 4.0 (http://www.cbs.dtu.dk/services/SignalP/) and WoLF PSORT (http://wolfpsort.org/), showed that RyAAAT3 does not contain signal peptides at its *N*-terminal, suggesting cytosolic localization.

RyAAAT3 preferred α-ketoglutaric acid as the amino-acceptor in the production of PPA than oxaloacetic acid

Optimum pH of enzyme was screened in a range of 7-10 by monitoring the production of PPA (Supplementary Fig. 3A). Also, the optimum temperature for the PPA production was determined and the highest at 45 ^{o}C was observed (Supplementary Fig. 3B). For RyAAAT3, α-ketoglutaric acid was the preferred amino acceptor rather than oxaloacetic acid in production of PPA from L-Phe under the optimum conditions in pH and reaction temperature conditions (Fig. 4A). Recombinant RyAAAT3 revealed the K_m and V_{max} values for the conversion of L-Phe with oxaloacetic acid were 0.73 ± 0.11 mM, 6.86 ± 0.04 nmol/mg protein/min,

341 respectively, and with α-keto-glutalic acid were 1.47 ± 0.37 mM, 21.85 ± 0.59

342 nmol/mg protein/min respectively (means ± SD; n=4).

343

344 RyAAAT3 preferred the forward reaction from L-Phe as a substrate to PPA than the

345 reverse reaction

346 To further characterize the enzymatic properties of RyAAAT3, we analyzed

347 relative activities of transamination reactions with several amino acids such as L-Phe,

348 D-phenylalanine, L-tyrosine and L-tryptophan. L-Phe gave the highest transaminase

349 activity, on the other hand L-tyrosine and L-tryptophan aromatic amino acids gave

350 one-fourth activity in comparison to L-Phe. RyAAAT3 hardly showed any activity for

351 substrates L-alanine, D-phenylalanine and glycine (Fig. 4B).

352 Aminotransferases catalyze *bi*-directional reactions in transamination. It was

353 proposed that L-Phe would be produced from PPA by aminotransferase in plants

354 (Maeda et al., 2011). We also determined the reaction selectivity of RyAAAT3 in

355 transamination. Forward reaction (L-Phe as a substrate, α-keto-glutalic acid as an

356 amino acceptor) and the reverse reaction (PPA and L-glutamic acid were used as an

357 acceptor and amino donor, respectively, under the same conditions as the forward

358 reaction) were evaluated by LC-MS analyses for the products (Supplementary Fig. 4).

359 The RyAAAT3 showed 9.7 fold higher transamination activity from L-Phe to PPA

(19.37 ± 0.67 pmol/mg protein/min) than reverse reaction (2.01 ± 0.47 pmol/mg protein/min). These results suggested that RyAAAT3 preferred L-Phe as a substrate compared to PPA.

Carbidopa inhibited transaminase activity of RyAAAT3

It is well known that aminotransferases form Schiff bases between the amino group of amino acid residue of aminotransferase and PLP. Also, rose AADC was reported to produce PAld with forming Schiff base. To confirm whether RyAAAT3 is PLP dependent enzyme or not, we quantified the production of PAld and PPA in AADC (decarboxylation) and AAAT (transamination) enzymatic assays with Carbidopa. Carbidopa inhibited production of PAld and PPA in concentration dependent manner and at 500 μM concentration PAld and PPA were hardly produced in the heterogeneously expressed rose AADC and RyAAAT3 (Fig. 5A,B).

RyAAAT was expressed in rose petals and various organs

We examined transcription level of *RyAAAT3* in various rose tissues at stage 4 by RT-PCR. *RyAAAT3* was expressed in rose petals and also other tissues, leaf, stem, rose hip and calyx (Fig. 6). The *C. melo AAAT* was expressed in similar manner in various organs, shoots, young and old leaves, and in immature fruits (Gonda et al.,

2010). Also, PAAS in petunia and AADC in tomato were expressed in various organs and not only in petals. The RyAAAT3 expressed in the petals may produce PPA from L-Phe in rose petals.

RNA interference of *RyAAAT3* suppressed 2PE production in the rose protoplasts

To elucidate the contributions of *RyAAAT3* to 2PE synthesis in the rose flowers, we performed RNAi experiments targeting *RyAAAT3* in the rose protoplasts. 2PE production in non-treated samples was almost the same as compared to control samples. RNAi experiments towards *RyAAAT3* decreased the 2PE production about 60% as compared to the control samples (Fig. 7). These results suggested *RyAAAT3* plays crucial role in 2PE biosynthesis of in rose flowers.

Discussion

Plant specialized (secondary) metabolites are biosynthesized in plants for survival in diverse ecological niches. These multitudes of chemicals are recognized as defense compounds against biotic and abiotic stresses and also as allelochemicals of other living organisms. Aromatic amino acids, L-tyrosine and L-Phe are initial compounds of the phenylpropanoid biosynthetic pathway leading to phenylpropanoids, lignans, lignins, stilbenes, coumarins, alkaloids and flavonoids. 2PE, a major

398 constituent of scent in many flowers and fruits is also derived from L-Phe. The
399 biological functions of 2PE have been considered as an antimicrobial agent and also
400 as a potent insect attractant (Pichersky and Gershenzon, 2002). Our previous
401 deuterium label feeding experiments in rose (*R.* 'Hoh-Jun' and *R. damascena* Mill.)
402 demonstrated four potential routes producing 2PE from L-Phe *via* i) PAld, ii)
403 phenethylamine, iii) *trans*-cinnamic acid/phenyllactate and iv) PPA (Erich pathway in
404 microorganism) (Hayashi et al., 2004). Tieman et al (2006) clearly showed that L-Phe
405 is decarboxylated to phenethylamine by a tomato AADC. Phenethylamine thus
406 produced is converted to PAld by removal of the amine group, followed by
407 conversion to 2PE by PAR, while one *bi*-functional enzyme decarboxylates and
408 deaminates L-Phe directly producing PAld in petunia and rose flower (Kaminaga et al.,
409 2006; Sakai et al., 2007). AADCs also play key roles in PAld production from L-Phe
410 in herbivory response and floral scent production in *Arabidopsis* plants (Gutensohn et
411 al., 2011).

412 In this report, we demonstrated an alternative route to convert L-Phe to PPA and
413 then PPA to PAld with crude enzymes from rose petals. These results indicated L-Phe
414 was converted to PAld *via* PPA in an enzymatic reaction in rose flowers. Also, we
415 were successful in detecting [$^2H_7$]PPA in rose petal protoplasts by feeding L-[$^2H_8$]Phe,
416 suggesting that the transamination of L-Phe to PPA is working *in vivo*. So far we could

417 not detect endogenous PPA in rose petal protoplasts by LC-MS. Similarly the
418 endogenous PPA was not determined in petunia though it was measurable after
419 feeding shikimic acid (Maeda et al., 2010). These results suggest that PPA is pretty
420 quickly converted to PAld in plants. Our conversion study here strongly suggested
421 that 2PE is biosynthesized from L-Phe *via* PPA in rose protoplasts and rose AAAT
422 forms PPA enzymatically from L-Phe. Although we have not identified genes
423 encoding the second step, PPA is presumably converted by a decarboxylase to PAld.
424 As isolated protoplasts are not physiologically and biochemically the same as the
425 flower petals, further investigations with rose petals are needed to confirm the actual
426 roles of AAAT and PPA in the 2PE biosynthesis. Although *RyAAAT3* was expressed in
427 the whole rose flower plant, 2PE concentrations were much lower in leaves, stems,
428 and calyxes than in flower petals (Oka et al., 1999). We need to investigate the role of
429 RyAAT3 in flowers, leaves, stems, and calyxes of the rose plants.

430 AAATs are classified in various AAAT families, such as phenylalanine
431 aminotransferases (PheATs) similarly to tyrosine aminotransferases (TyrATs) and
432 tryptophan aminotransferases (TrpATs) and several reports concerning enzymatic
433 characterizations of AAATs have been published (Lopukhina et al., 2001; Stepanova
434 et al. 2008; Tao et al., 2008; Prabhu and Hudson, 2010; Gonda et al., 2010; Lee and
435 Facchini, 2011). *Arabidopsis WEAK ETHYLENE INSENSITIVE8* (*WEI8*) gene family

436 link the tissue-specific effects of ethylene and auxin production (Stepanova et al.,
437 2008) and the shade avoidance response of plants to low red/far-red light is essential
438 for the expression of *SHADE AVOIDANCE3* (*SAV3*) gene (Tao et al., 2008). These
439 two genes, *WEI8* and *SAV3*, encode a TrpAT that catalyzes the conversion of
440 tryptophan to indole-3-pyruvic acid, an intermediate in auxin biosynthetic pathway.
441 Functional characterization of the *Arabidopsis* the locus tags At4g23600 and
442 At5g36160, annotated as TyrAT, revealed that the enzymes form 4-
443 hydroxyphenylpyruvate from L-Tyr. There are a few reports that plant AAATs convert
444 L-Phe to PPA, but the transamination activities for L-Phe of reported plant AAATs are
445 quite low compared to the reaction preferred substrate (Lee and Facchini, 2011). The
446 existence of specific PheAT has remained unclear despite substantial efforts. Very
447 recently, a novel PheAT gene in melon was isolated and characterized (*C. melo*
448 AAAT) encoding 45.6 kDa protein. *C. melo* AAAT catalyzed the transamination of L-
449 Phe and L-Tyr to PPA and 4-hydroxyphenylpyruvic acid, respectively. With low
450 turnovers *Arabidopsis* TyrAT (At5g36160) also formed PPA from L-Phe (Prabhu and
451 Hudson, 2010). Our cloned RyAAAT3 showed high similarity with *C. melo* AAAT at
452 78% and with *Arabidopsis* TyrAT (At5g36160) at 74%, whereas RyAAAT3 showed
453 relatively low similarity with *Arabidopsis WEI8*/*SAV3* (TrpAT) and poppy TyrAT (Lee
454 and Facchini, 2011) at 50-60%. A phylogenetic analysis showed that RyAAATs and

some aminotransferases were classified into three clades, AspAT, AlaAT and aminotransferases specific to aromatic amino acids, based on their amino acid sequences (Supplementary Fig. 5). Similar to RyAAAT3, *C. melo* AAAT expressed in *E. coli* preferred L-Phe as a substrate by 3.5 fold higher than L-tyrosine. We here propose that the RyAAAT3 and the *C. melo* AAAT are 'phenylalanine aminotransferases' within the AAAT clade as these aminotransferases were only reported to have the preference for L-Phe as a substrate. A Blast search in the plant EST database (TIGR Plant Transcript Assembly BLAST Server, http://plantta.jcvi.org/index.shtml) identified EST clones with homology to RyAAAT3 in various plants such as *Arabidopsis thaliana*, *Medicago truncatula*, *Solanum lycopersicum* (tomato), *Helianthus annuus* (sunflower), *Fragaria vesca* (woodland strawberry), *Malus x domestica* (cultivated apple), *Glycine max* (soybean), *Vitis vinifera* (wine grape), *Coffea canephora* (coffee robusta), *Gossypium raimondii*, *Solanum tuberosum* (potato) and *Brassica napus* (oilseed rape). Although these ESTs are annotated as a TyrAT because a PheAT is very newly reported, this Blast search indicates the possibility that PheAT are widely distributed throughout the plant kingdom.

Enzymatic findings demonstrated that 2PE is biosynthesized *via* different pathway compared to previous reports on tomato, petunia and rose. This study is the

first report establishing that rose protoplasts utilize two different 2PE biosynthetic pathways and that L-Phe is converted to PAld *via* PPA to produce 2PE. It remains unclear why rose flowers utilize two different 2PE biosynthetic pathways. We need to quantify the contribution of RyAAAT3 in 2PE production in the flowers of *R.* 'Yves Piaget'.

Rose AADC may be involved in reproduction process in rose. It reported that the potential biological function of Arabidopsis TyrAT is the defense response to herbivores and pathogens (Song et al., 2004a,b). The mRNAs of Arabidopsis TyrAT could be induced by various octadecanoids and by wounding of the plants and accumulation of the Arabidopsis TyrAT protein was observed after application of chemical and physical stresses (Lopukhina et al., 2001). Moreover, Song et al (2004) demonstrated that two aminotransferases, AGD2 (At4g33680) and ALD1 (At2g13810) is integral genes in the biosynthesis of phytopathogen resistance chemicals. These findings proposed that RyAAAT3 may play an important role in resistance against various environment stresses in rose, although further investigations are needed.

Acknowledgments

We thank Drs. S. Baldermann, V. K. Deo, Z.Y. Yang for informative discussion and

critical reading of this manuscript. We also thank Ichikawa Rosary for supplying the roses throughout our study and Ms. Y. Ryuno for technical support. The work is supported in part by the Grand-in-Aid for Scientific Research (B), JSPS to N.W.

References

An CI, Sawada A, Fukusaki E, Kobayashi A. A transient RNA interference assay system using Arabidopsis protoplasts. Biosci Biotechnol Biochem 2003;67:2674-7.

An CI, Sawada A, Kawaguchi Y, Fukusaki E, Kobayashi A. Transient RNAi induction against endogenous genes in Arabidopsis protoplasts using in vitro-prepared double-stranded RNA. Biosci Biotechnol Biochem 2005;69:415-8.

Aubert C, Baumann S, Arguel H. Optimization of the analysis of flavor volatile compounds by liquid–liquid microextraction (LLME). Application to the aroma analysis of melons, peaches, grapes, strawberries, and tomatoes. J Agric Food Chem 2005;53:8881–95.

Bertoldi M, Gonsalvi M, Contestabile R, Voltattorni CB. Mutation of tyrosine 332 to phenylalanine converts dopa decarboxylase into a decarboxylation-dependent oxidative deaminase. J Biol Chem 2002;277:36357-62.

Burkhard P, Dominici P, Borri-Voltattorni C, Jansonius JN, Malashkevich VN. Crystal

512 structure and substrate specificity of drosophila 3,4-dihydroxyphenylalanine
513 decarboxylase. Nat Struct Biol 2001;8:963–967.
514 Chen XM, Kobayashi H, Sakai M, Hirata H, Asai T, Ohnishi T, Baldermann S,
515 Watanabe N. Functional characterization of rose phenylacetaldehyde reductase
516 (PAR), an enzyme involved in the biosynthesis of the scent compound 2-
517 phenylethanol. J Plant Physiol 2011;168: 88-95.
518 Dorman DC, Struve MF, Norris A, Higgins AJ. Metabolomic analyses of body fluids
519 after subchronic manganese inhalation in rhesus monkeys. Toxicological Sci
520 2008;106:46-54.
521 Ehrlich F. Über die Bedingungen der Fuselölbildung und über ihren Zusammenhang
522 mit dem Eiweißaufbau der Hefe. Berichte der Deutschen Chemischen
523 Gesellschaft 1907;40:1027-47.
524 Gonda I, Bar E, Portnoy V, Lev S, Burger J, Schaffer AA, Tadmor Y, Gepstein S,
525 Giovannoni JJ, Katzir N, Lewinsohn E. Branched-chain and aromatic amino acid
526 catabolism into aroma volatiles in *Cucumis melo* L. fruit. J Exp Bot
527 2010;61:1111-23.
528 Gutensohn M, Klempien A, Kaminaga Y, Nagegowda DA, Negre-Zakharov F, Huh
529 JH, Luo H, Weizbauer R, Mengiste T, Tholl D, Dudareva N. Role of aromatic
530 aldehyde synthase in wounding/herbivory response and flower scent production

in different Arabidopsis ecotypes. Plant J 2011;66:591-602.

Guterman I, Shalit M, Menda N, Piestun D, Dafny-Yelin M, Shalev G, Bar E, Davydov O, Ovadis M, Emanuel M, Wang J, Adam Z, Pichersky E, Lewinsohn E, Zamir D, Vainstein A, Weiss D. Rose scent: genomics approach to discovering novel floral fragrance-related genes. Plant Cell 2002;14:2325-38.

Hayashi S, Yagi K, Ishikawa T, Kawasaki M, Asai T, Picone J, Turnbull C, Hiratake J, Sakata K, Takada M, Ogawa K, Watanabe N. Emission of 2-phenylethanol from its β-D-glucopyranoside and the biogenesis of these compounds from [$^2H_8$] L-phenylalanine in rose flowers. Tetrahedron 2004;60: 7005–13.

Hua D, Xu P. Recent advances in biotechnological production of 2-phenylethanol. Biotechnol Advances 2011;29:654-60.

Huang B, Yi B, Duan Y, Sun L, Yu X, Guo J, Chen W. Characterization and expression profiling of tyrosine aminotransferase gene from *Salvia miltiorrhiza* (Dan-shen) in rosmarinic acid biosynthesis pathway. Mol Biol Rep 2008;35:601-12.

Kaminaga Y, Schnepp J, Peel G, Kish CM, Ben-Nissan G, Weiss D, Orlova I, Lavie O, Rhodes D, Wood K, Porterfield DM, Cooper AJ, Schloss JV, Pichersky E, Vainstein A, Dudareva N. Plant phenylacetaldehyde synthase is a bifunctional homotetrameric enzyme that catalyzes phenylalanine decarboxylation and

oxidation. J Biol Chem 2006;281: 23357-66.

Lee EJ, Facchini PJ. Tyrosine aminotransferase contributes to benzylisoquinoline alkaloid biosynthesis in opium poppy. Plant Physiol 2011;157:1067-78.

Lopukhina A, Dettenberg M, Weiler EW, Holländer-Czytko H. Cloning and characterization of a coronatine-regulated tyrosine aminotransferase from Arabidopsis. Plant Physiol 2001;126:1678-87.

Maeda H, Shasany AK, Schnepp J, Orlova I, Taguchi G, Cooper BR, Rhodes D, Pichersky E, Dudareva N. RNAi suppression of Arogenate Dehydratase1 reveals that phenylalanine is synthesized predominantly via the arogenate pathway in petunia petals. Plant Cell 2010;22:832-49.

Maeda H, Yoo H, Dudareva N. Prephenate aminotransferase directs plant phenylalanine biosynthesis via arogenate. Nat Chem Biol. 2011;7:19-21.

Oka N, Shimosato I, Ohishi H, Hatano T, Günata Z, Baumes R, Sakata K, Watanabe N. Glycosidic aromas and glycohydrolases being involved in potentially aroma formation in rose flowers of two different species. J Essential Oil-Bearing Plants 1999: 2:91-100.

Marilley L, Casey MG. Flavours of cheese products: metabolic pathways, analytical tools and identification of producing strains. International J Food Microbiol 2004;90:139–59.

569 Pichersky E, Gershenzon J. The formation and function of plant volatiles: perfumes
570 for pollinator attraction and defense. Curr Opin Plant Biol 2002;5:237-43.
571 Prabhu PR, Hudson AO. Identification and Partial Characterization of an L-Tyrosine
572 Aminotransferase (TAT) from Arabidopsis thaliana. Biochem Res Int
573 2010;2010:549572.
574 Sakai M, Hirata H, Sayama H, Sekiguchi K, Itano H, Asai T, Dohra H, Hara M,
575 Watanabe N. Production of 2-phenylethanol in roses as the dominant floral scent
576 compound from L-phenylalanine by two key enzymes, a PLP-dependent
577 decarboxylase and a phenylacetaldehyde reductase. Biosci Biotechnol Biochem
578 2007;71:2408-19.
579 Sayama H. Chemical synthesis of ^{13}C-shikimic acid and its metabolism in rose petals.
580 Master dissertation, Shi-zuoka University, Japan 2008 [in Japanese].
581 Schwab W, Davidovich RR, Lewinsohn E. Biosynthesis of plant-derived flavor
582 compounds. Plant J 2008;54:712–32.
583 Sheen J. Signal transduction in maize and *Arabidopsis* mesophyll protoplasts. Plant
584 Physiol 2001;127:1466-75.
585 Song JT, Lu H, Greenberg JT. Divergent roles in Arabidopsis thaliana development
586 and defense of two homologous genes, aberrant growth and death2 and AGD2-
587 LIKE DEFENSE RESPONSE PROTEIN1, encoding novel aminotransferases.

588 Plant Cell 2004a;16:353-66.
589 Song JT, Lu H, McDowell JM, Greenberg JT. A key role for ALD1 in activation of
590 local and systemic defenses in Arabidopsis. Plant J 2004b;40:200-12.
591 Stepanova AN, Robertson-Hoyt J, Yun J, Benavente LM, Xie DY, Dolezal K,
592 Schlereth A, Jürgens G, Alonso JM. TAA1-mediated auxin biosynthesis is
593 essential for hormone crosstalk and plant development. Cell 2008;133:177-91.
594 Tadmor Y, Fridman E, Gur A, Larkov O, Lastochkin E, Ravid U, Zamir D, Lewinsohn
595 E. Identification of malodorous, a wild species allele affecting tomato aroma that
596 was aelected against during domestication. J Agric Food Chem 2002;50:2005-9.
597 Tao Y, Ferrer JL, Ljung K, Pojer F, Hong F, Long JA, Li L, Moreno JE, Bowman ME,
598 Ivans LJ, Cheng Y, Lim J, Zhao Y, Ballaré CL, Sandberg G, Noel JP, Chory J.
599 Rapid synthesis of auxin via a new tryptophan-dependent pathway is required for
600 shade avoidance in plants. Cell 2008;133:164-76.
601 Tieman DM, Taylor M, Schauer N, Fernie AR, Hanson AD, Klee HJ. Tomato
602 aromatic amino acid decarboxylases participate in synthesis of the flavor volatiles
603 2-phenylethanol and 2-phenylacetaldehyde. Proc Natl Acad Sci U S A
604 2006;103:8287-92.
605 Tieman DM, Loucas HM, Kim JY, Clark DG, Klee HJ. Tomato phenylacetaldehyde
606 reductases catalyze the last step in the synthesis of the aroma volatile 2-

phenylethanol. Phytochemistry 2007;68:2660-9.

Yang Z, Sakai M, Sayama H, Shimeno T, Yamaguchi K, Watanabe N. Elucidation of the biochemical pathway of 2-phenylethanol from shikimic acid using isolated protoplasts of rose flowers. J Plant Physiol 2009;166:887-91.

Yennawar N, Dunbar J, Conway M, Hutson S, Farber G. The structure of human mitochondrial branched-chain aminotransferase. Acta Crystallogr D Biol Crystallogr 2001;57:506-15.

Legends of figures

Fig. 1. Hypothesized biosynthetic pathway and determination of [$^2H_7$]PPA production in rose protoplasts. (A) AADC route (grey arrow) and proposed AAAT route (solid arrow) for the production of 2PE from L-Phe in the isolated protoplasts of *R.* 'Yves Piaget'. The novel AAAT-route involves the hypothetical intermediate PPA and the enzyme RyAAAT. (B) Typical rose petal protoplasts. (Scale bar in 20 μm). (C) LC-MS chromatogram of [$^2H_7$]PPA in protoplasts. [$^2H_7$]PPA (*m/z* 170 [M-H]$^-$, with asterisk) was detected at a retention time (6.66 min), which was identical to that of authentic PPA (asterisk, *m/z* 163 [M-H]$^-$). [$^2H_7$]PPA was not detected in the protoplasts without (w/o) L-[$^2H_8$]Phe feeding.

626

627 Fig. 2. Conversion of L-Phe to PPA and PPA to PAld with a crude enzyme extract. (A)
628 LC-MS chromatograms of L-Phe conversion to PPA. (B) GC-MS chromatograms of
629 PPA conversion to PAld. PPA (retention time = 6.66 min) was traced at *m/z* 163 [M-
630 H]$^-$ on LC-MS, and PAld (retention time = 4.56 min) was traced at *m/z* 120 [M]$^+$ by
631 GC-MS. The asterisks indicated peaks of PPA (A) and PAld (B), respectively.
632 Negative control stands for the chromatograms of the reaction mixtures at the
633 beginning of the enzymatic reaction. PAld production from PPA by chemical
634 conversion was negligible during the incubation period.

635

636 Fig. 3. Heterogeneous expression and transaminase activity of RyAAAT3. (A) SDS-
637 PAGE of samples used in the RyAAAT3 activity analysis and the image of RyAAAT3
638 visualized by Ag-staining (lane 1-3) and His-tag-specific reagent (His-Detect In-Gel
639 Stain, Nacalai Tesque, Kyoto Japan) (lanes 4 and 5). Lane 1, protein molecular
640 markers; lanes 2 and 4, empty vector; lanes 3 and 5, purified recombinant RyAAAT3
641 protein (arrow). (B) LC-MS chromatogram of enzymatic product of RyAAAT3. PPA
642 (asterisks) was detected at 6.66 min on the LC-MS chromatogram monitored at *m/z*
643 163 [M-H]$^-$. Negative control on Fig. 3B indicates the LC-MS chromatogram
644 monitored at *m/z* 163 [M-H]$^-$ for the reaction mixture at beginning of the reaction in

645 the presence of L-Phe and RyAAAT3.

646

647 Fig. 4. Characterization of RyAAAT3 in amino acceptor preference and substrate
648 specificity. (A) RyAAAT3 kinetics with oxaloacetic acid (open circle) or α-
649 ketoglutaric acid (closed circle). (B) Relative conversion of selected amino acids to
650 their keto-acids, catalyzed by RyAAAT3. (Abbreviations are as follows: L-Phe; L-
651 Phenylalanine, L-Trp, L-Tryptophan; L-Tyr, L-Tyrosine; D-Phe; D-Phenylalanine, Gly;
652 Glycine, L-Ala; L-Alanine). Relative activities were determined under L-Phe V_{max}
653 conditions. The activity (21.85 ± 0.59 nmol/mg protein/min) with L-Phe was taken at
654 100%. Amino acids were used at equal concentrations of 10 mM. N.D. means not
655 detected. Error bars represent standard deviation (SD, n=3).

656

657 Fig. 5. Inhibition of PLP-dependent enzymes, rose AADC and RyAAAT3. PAld (A)
658 and PPA (B) productions were examined in the presence of Carbidopa based on the
659 GC-MS and LC-MS analyses, respectively. The amounts of PAld and PPA in the
660 absence of Carbidopa were taken as 1.0 for control group (CNT). N.D. means not
661 detected. The relative rates were calculated based on the averages of three replicates ±
662 SD.

663

Fig. 6. Transcriptional analysis of *RyAAAT3* in various organs of *R.* 'Yves Piaget'. Total RNA was extracted from tissues of 3 independent *R.* 'Yves Piaget' plants. RT-PCR of 18S ribosomal RNA was used as a house keeping gene. *RyAAAT3* primers for transcriptional analysis are listed in Supplementary Table 1.

Fig. 7. Effect of RNAi-mediated silencing of *RyAAAT3* in protoplasts. The 2PE synthesis was measured in protoplasts prepared from rose petals. The control (CNT) and knockdown groups (RyAAAT3 K/D) were treated with PEG-Ca solution, and the NT groups were not treated. Statistics analysis was performed in student *t*-test. The amount (15 nmol/10^5 protoplast cells) of 2PE production for CNT was taken as 1.0. The relative rates were calculated based on the averages of 2PE amounts in the CNT group and the data were obtained from three independent replicates ± SD.

Supplementary Information

Material and methods

Preparation of crude enzymes from the flowers of *R.* 'Yves Piaget'

The rose petals were crushed in liquid nitrogen, and lyophilized to obtain powdered material. For the L-Phe conversion, this material (0.7 g) was homogenized in 0.1 M Tris-HCl buffer pH 8.0 containing 0.1 mM PLP, 1 mM EDTA, 1% glycerol and 0.1% TritonX-100 in the presence of 5.3 g PVPP (Polyclar 10, ISP Japan). After centrifugation (26,000*g*, 15 min, 4 ^{o}C), the proteins in the supernatant were precipitated with ammonium sulfate (0-80%). Then additional centrifugation (26,000*g*, 30 min, 4 ^{o}C) gave the pellets, and it was dissolved in Tris-HCl buffer pH 8.0 containing 0.1 mM PLP, 1 mM EDTA and 1% glycerol and supplied to transaminase assay with L-Phe as the substrates and α-keto-glutalic acid as described below. For the PPA conversion, the powdered material (1.0 g) was homogenized in 0.1 M citrate buffer pH 6.0 containing 1% TritonX-100 in the presence of 5.7 g PVPP. After centrifugation (26,000 *g*, 15 min, 4 ^{o}C), 100 μL the supernatant and 50 mM PPA (2.5 μmol) in a 0.1 M citrate buffer pH 6.0 were incubated at 35 ^{o}C for 2 h and then ethyldecanoate in methanol (1.55 nmol) was added as an internal standard. The volatiles were extracted with 400 μL of hexane:ethyl acetate (1:1, v/v). The organic layer was dried over Na_2SO_4 and subjected to GC-MS analyses. The GC-MS conditions are as shown in the paragraph 'GC-MS analysis'.

GC-MS analysis

Analyses of 2PE and PAld were performed using a GC-MS QP5050 (Shimadzu), which was controlled by a Class-5000 work station. For the analyses of 2PE, the GC was equipped with a capillary TC-WAX column (GL Sciences Inc., Japan) of 30 m × 0.25 mm I.D. and 0.25 μm film thickness. For the analysis of PAld, the GC was equipped with a capillary TC-5 column (30 m × 0.25 mm I.D., 0.25 μm film thickness, GL Sciences Inc., Japan).

For 2PE analysis, the column temperature was elevated from 60 ^{o}C (3 min hold) to 180 ^{o}C (40 ^{o}C /min) then to 240 ^{o}C (10 ^{o}C/min, 3 min hold). The injector temperature was 200 ^{o}C, the ionizing voltage was 70 eV, and the scanning speed was 0.5 scan/s with a range of *m/z* 76–200. For PAld analysis, the column temperature was elevated from 50 ^{o}C (3 min hold) to 90 ^{o}C (10 ^{o}C/min), then to 130 ^{o}C (30 ^{o}C/min) and then 290 ^{o}C (40

^{o}C/min, 3 min hold). The injector temperature, the ionizing voltage, the scanning speed, and the *m/z* range were the same as for the 2PE analysis.

Substrate specificity of RyAAAT3

The reaction was initiated by the addition of the amino acid and performed at 45 ^{o}C under V_{max} conditions for L-Phe. The reaction was stopped by adding an equal volume acetonitrile after adding 200 nmol L-[$^{2}H_{8}$]Phe as the internal standard. The sample was subjected to centrifugation (20,000 *g*, 10 min, 4 ^{o}C), filtered (Millex LH, Millipore) and subsequently analyzed by LC-MS (L, D-Phe, L-tyrosine, L-tryptophan) and an amino acid analyzer (Hitachi) (L-alanine and glycine). The products, PPA, 4-hydroxyphenylpyruvic acid and indole-3-pyruvic acid, were identified by comparing with the authentic specimens. The decrease in L-alanine and glycine were determined by amino acid analyzer following the manufacturing instructions.

Supplementary Table

Supplementary Table 1. Primers used in this study. A primer in QuantumRNA Universal 18S Internal Standard kit (Ambion) was used for 18srRNA.

Primers	sequence (5' - 3')
3' RACE PCR	
RyAAAT1	GCITAYCARGGITTYGCIW
RyAAAT2	CTCGGACAGAAGCCTCTAAC
RyAAAT3	CCATGGAGAATGGAACCCATG
5' RACE PCR	
RyAAAT1 for PCR	TGCTCCGGGTTCGATCCTG
RyAAAT1 for nested PCR	TCAAACAGCTGATGTCGCA
RyAAAT2 for PCR	CAGTTCGCAGTTTCTTCCAGG
RyAAAT2 for nested PCR	GTGGAACTGGAACCAGAACC
Full length PCR	
RyAAAT1 Forward	ATGAACTCACTCTCCGCTTCC
RyAAAT1 Reverse	TTAAGCAAGACGAGTAACAGC
RyAAAT2 Forward	CACAGCAATCATGCCACCG
RyAAAT2 Reverse	TTACATCCTTGAATAGCCTCTG
Subcloning to pET28a	
RyAAAT1 Forward (BamHⅠ)	GTGGGATCCATGAACTCACTCTCCGCTTC
RyAAAT1 Reverse (XhoⅠ)	ATACTCGAGAGCAAGACGAGTAACAGCTGC
RyAAAT2 Forward (EcoRⅠ)	GTGGAATTCATGCCACCGAAGGCATTGGAC
RyAAAT2 Reverse (SalⅠ)	GTGGTCGACCATCCTTGAATAGCCTCTGTC
RyAAAT3 Forward (SalⅠ)	GTGGTCGACGCATGGAGAATGGAACCCATGTG
RyAAAT3 Reverse (XhoⅠ)	GCGCTCGAGTAATTTTCTGGCATGCCTTTG
Transcripts analysis	
RyAAAT3 transcripts analysis Forward	CACTGTGGGTCTTCCGCAAAC
RyAAAT3 transcripts analysis Reverse	TCCCAAGGATGCTCGGAACTG
dsRNA synthesis	
RyAAAT3-N terminal T7 promoter	TAATACGACTCACTATAGGGATAAACCCCGGAAATCCTTG
RyAAAT3-N terminal	ATAAACCCCGGAAATCCTTG
RyAAAT3-C terminal T7	TAATACGACTCACTATAGGGAATGGTTTATCCC

promoter	CAAAGGC
RyAAAT3-C terminal	AATGGTTTATCCCCAAAGGC

Supplementary Figures

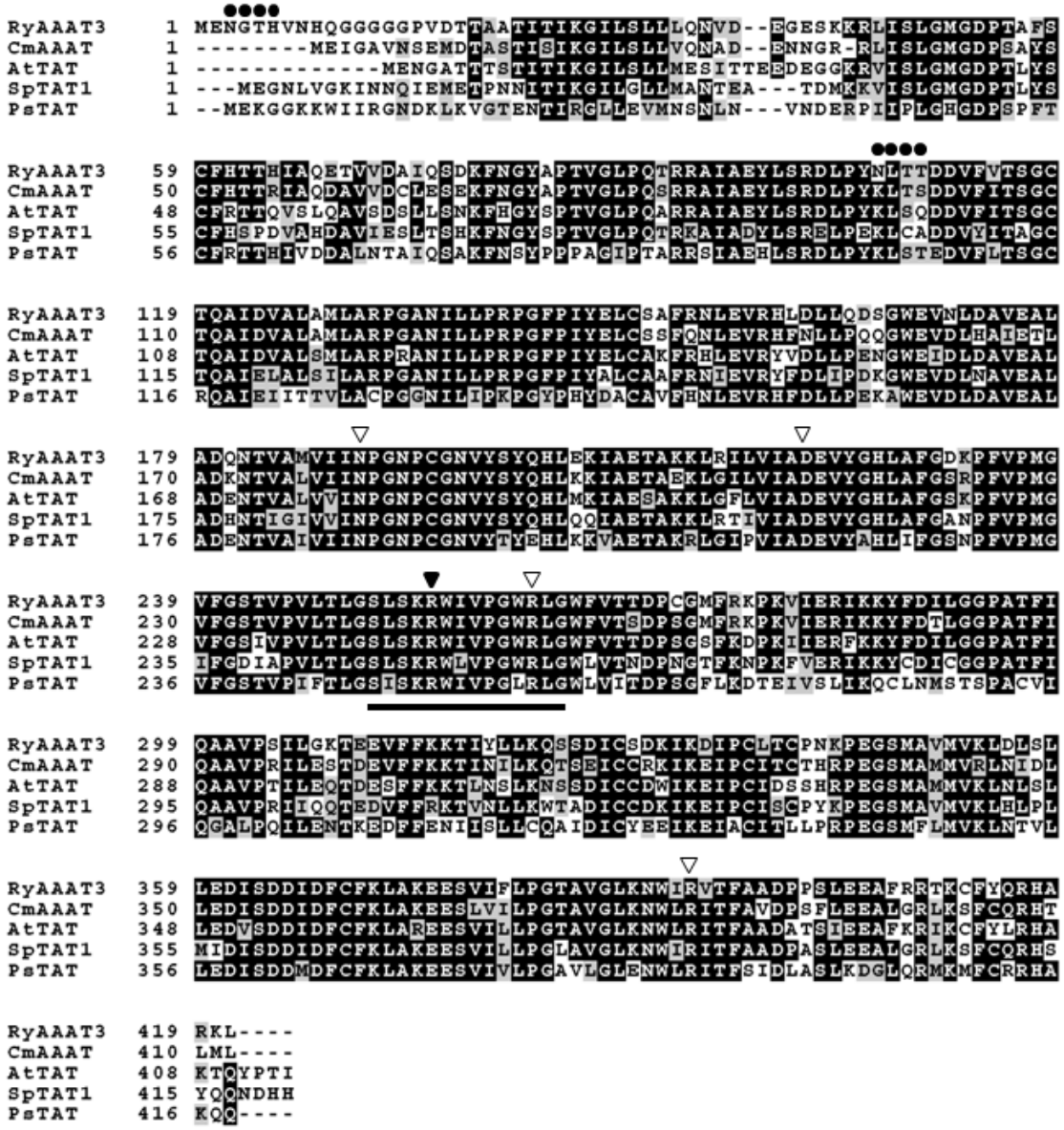

Supplementary Fig. 1. Amino acid sequence multiple alignments of RyAAAT3 and plant AAAT/TyrAT. *Cucumis melo* L. AAAT (CmAAAT, ADC45389), *Papaver somniferum* TyrAT (PsTAT, ADC33123), *Solanum pennellii* TyrAT 1 (SpTAT, ADZ24702) and *Arabidopsis thaliana* TyrAt (AtTAT, NP_200208). Black arrowheads indicate the conserved Lys residues that covalently bind the PLP cofactor and white arrowheads indicate conserved amino acids proposed to possess crucial roles in catalysis (Blankenfeldt et al., 1999; Yennawar et al., 2001). Underline shows

aminotransferases family-I PLP attachment site. Black dots indicate *N*-glycosylation site predicted in Genetyx version 8.0 software.

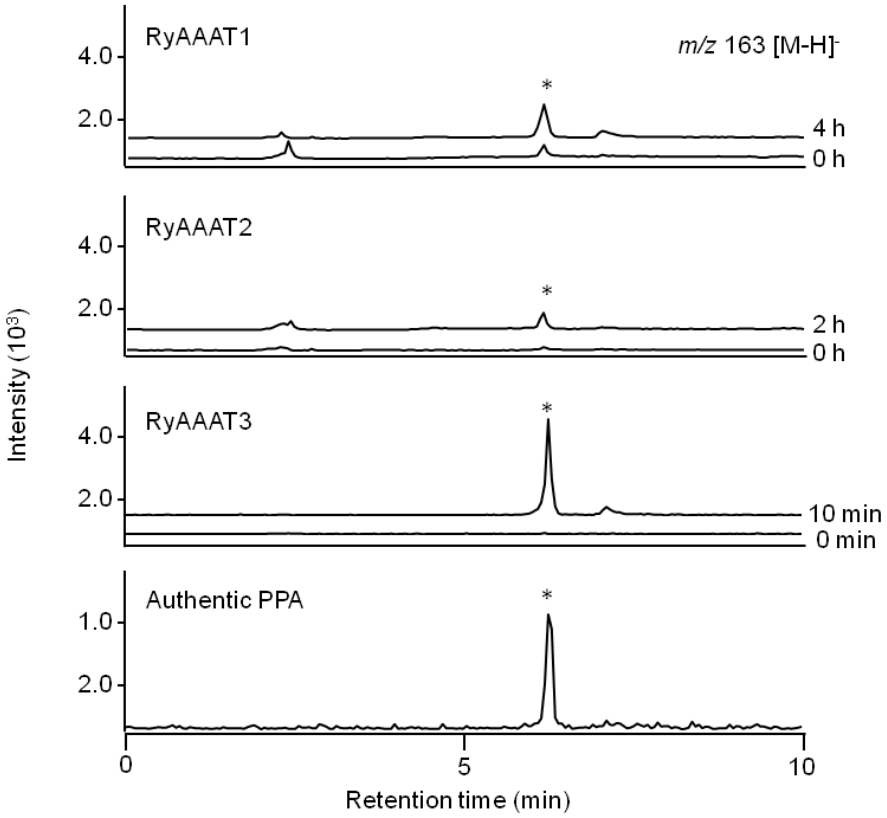

Supplementary Fig. 2. Comparison of transaminase activity among RyAAAT1-3. Selected ion traces at *m/z* 163 $[M-H]^-$ on LC-MS analyses of L-Phe metabolites produced with recombinant RyAAAT1-3 extracted from *E. coli* cultures. The asterisks depict peaks for authentic PPA and PPA detected in each respective chromatogram. PPA production was not detectable in RyAAAT1 and 2 reaction mixtures after 10 min reaction time.

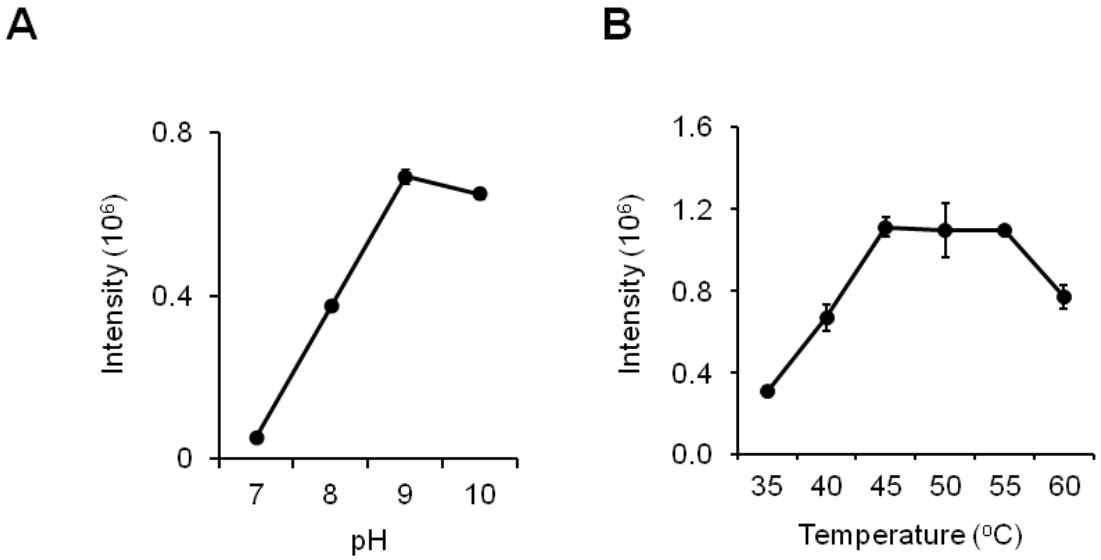

Supplementary Fig. 3. Characterization of RyAAAT3 enzymatic parameters. (A) Optimum pH; (B) Optimum temperature of the transaminase reaction producing PPA from L-Phe with α-ketoglutaric acid as an amino acceptor. (mean of 3 replicates ± SD).

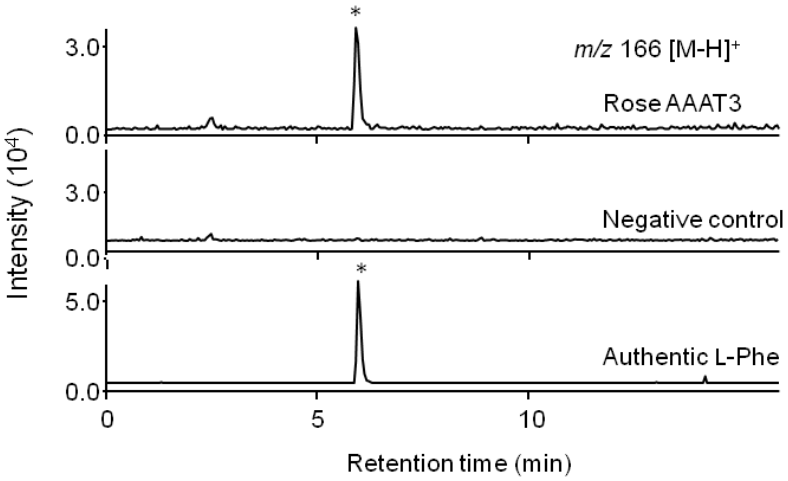

Supplementary Fig. 4. LC-MS chromatogram of PPA conversion to L-Phe, reverse reaction of RyAAAT3. RyAAAT3 transaminates PPA with L-glutamic acid as an amino donor. Negative control stands for beginning of the reaction. The asterisk depicts peak for authentic L-Phe and that detected in the reaction mixtures. Retention time of L-Phe was 5.98 min. Reaction mixtures (150 µL) containing 10 mM PPA, 10 mM L-glutamic acid, and 30 µL enzyme solution in a 0.5 M Tris-HCl buffer (pH 9.0) was incubated at 45 ^{o}C for 10 min. The reaction was stopped by adding equal volumes acetonitrile after adding 200 nmol L-[$^{2}H_{8}$]Phe as an internal standard. After the sample was centrifuged (20,000*g*, 10 min, 4 ^{o}C), the supernatant was filtered (Millex LH, Millipore) and analyzed by LC-MS.

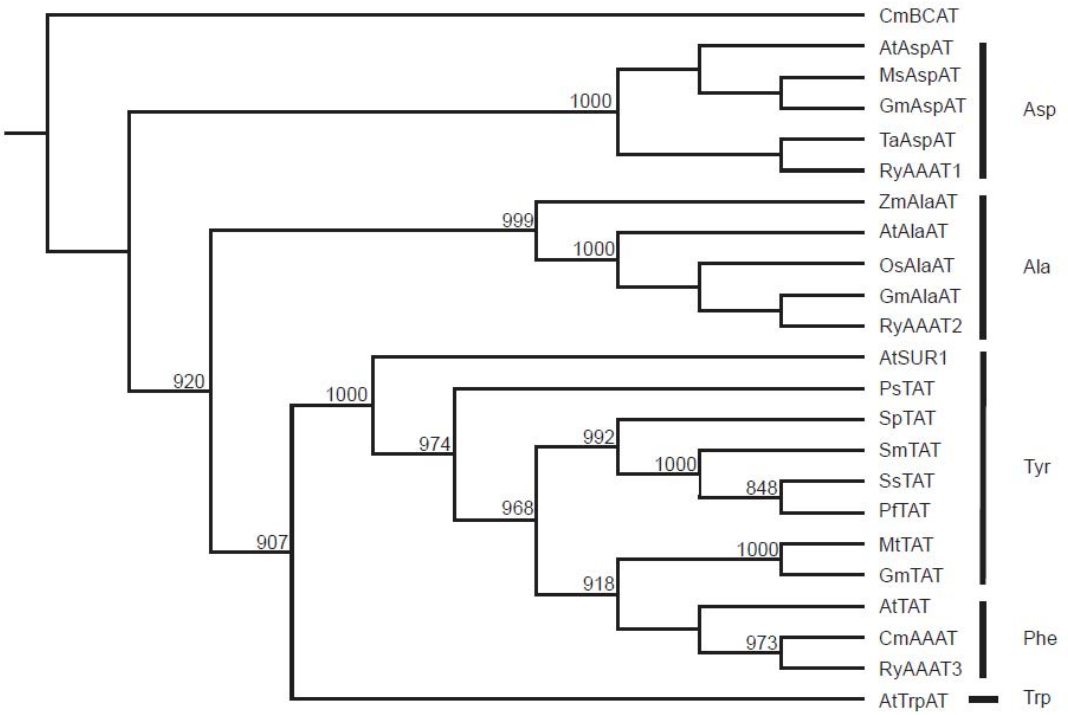

Supplementary Fig. 5. A phylogenetic tree of members of RyAAATs and AspATs, AlaATs, TrpATs, TyrATs and SUPERROOT 1 are from various plants. The multiple alignments of AAATs were performed with ClustalW 1.81. (Abbreviations are as follows: At, *Arabidopsis thaliana*; Cm, *Cucumis melo* (melon); Gm, *Glycine max*; Ms, *Medicago sativa*; Mt, *Medicago truncatula*; Os, *Oryza sativa*; Pf, *Perilla frutescens*; Ps, *Papaver somniferum*; Ry, *Rosa* 'Yves Piaget'; Sm, *Salvia miltiorrhiza*; Sp, *Solanum pennellii* (tomato); Ss, *Solenostemon scutellarioides*; Ta, *Triticum aestivum*; Zm, *Zea mays*; BCAT, branched chain aminotransferase; SUR1, SUPERROOT 1 (similar to TyrAT). A molecular phylogenetic tree was constructed by the neighbor-joining (NJ) method. The statistical significance of the NJ tree topology was evaluated by bootstrap analysis 1,000 iterative tree construction. The tree was drawn with CLC Sequence Viewer 6. Bootstrap values (1000 replicates) are given for the nodes. Bootstrap values over 800 are shown. All listed aminotransferases are as follows: AtTrpAT, NP177213; AtTAT, NP200208; GmTAT, AAY21813; MtTAT, AAY85183; SpTAT1, ADZ24702; SmTAT, ABC60050; PfTAT, ADO17550; SsTAT, CAD30341; PsTAT, ADC33123; AtSUR1, Q9SIV0; CmAAAT, ADC45389; CmBCAT, ADC45390; GmAspAT, AAC50015; MsAspAT, CAA43779; AtAspAT, NP196713; TaAspAT, ABY58643; GmAlaAT, ABW17197; AtAlaAT, NP177215; OsAlaAT, AAO84040; ZmAlaAT,

AAC62456.

References

Blankenfeldt W, Nowicki C, Montemartini-Kalisz M, Kalisz HM, Hecht HJ. Crystal structure of *Trypanosoma cruzi* tyrosine aminotransferase: substrate specificity is influenced by cofactor binding mode. Protein Science 1999;8:2406-17.

Yennawar N, Dunbar J, Conway M, Hutson S, Farber G. The structure of human mitochondrial branched-chain aminotransferase. Acta Crystallogr D Biol Crystallogr 2001;57:506-15.